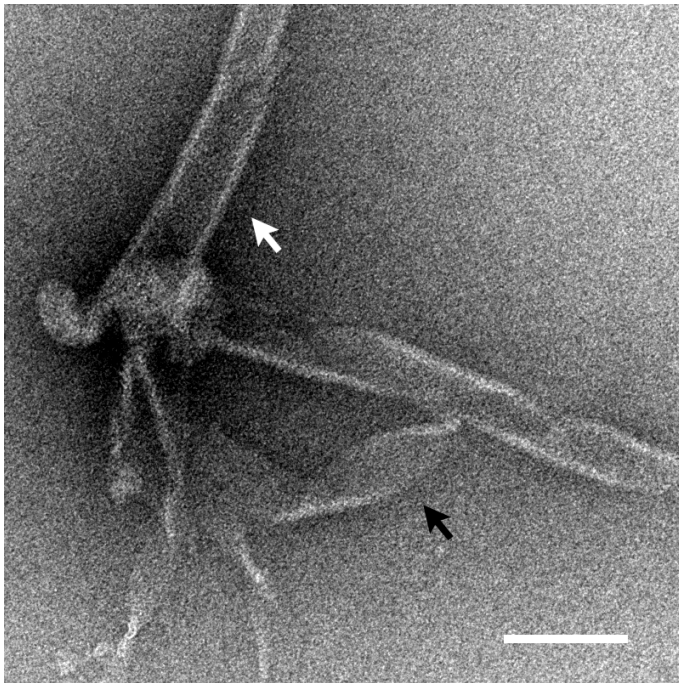
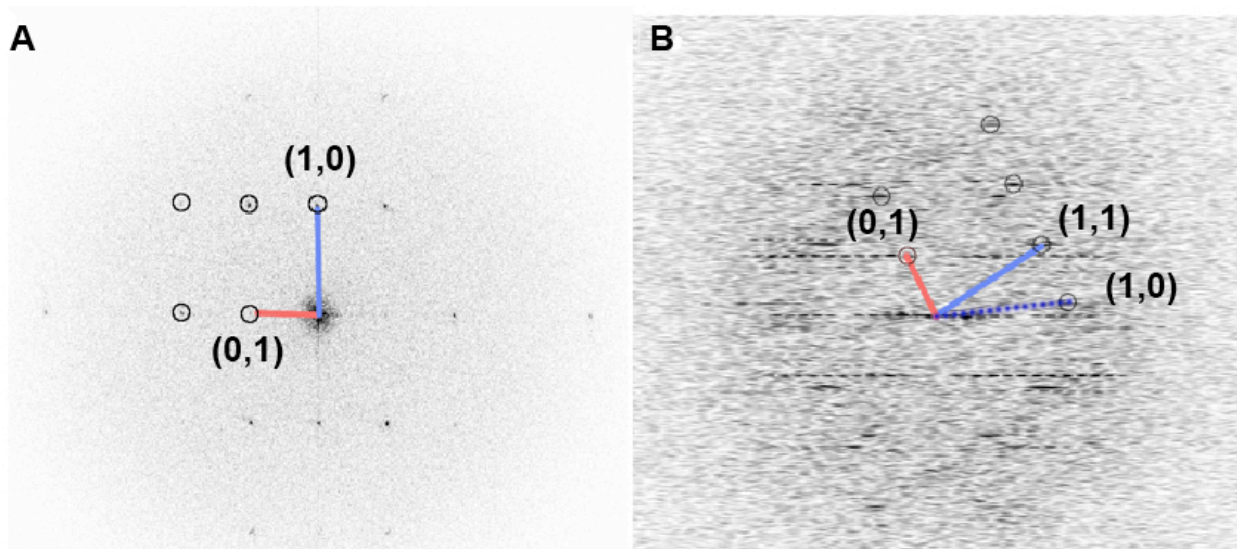


## Supplementary Materials

### Surface for Catalysis by Poliovirus RNA-Dependent RNA Polymerase, by Wang, Lyle, Bullitt



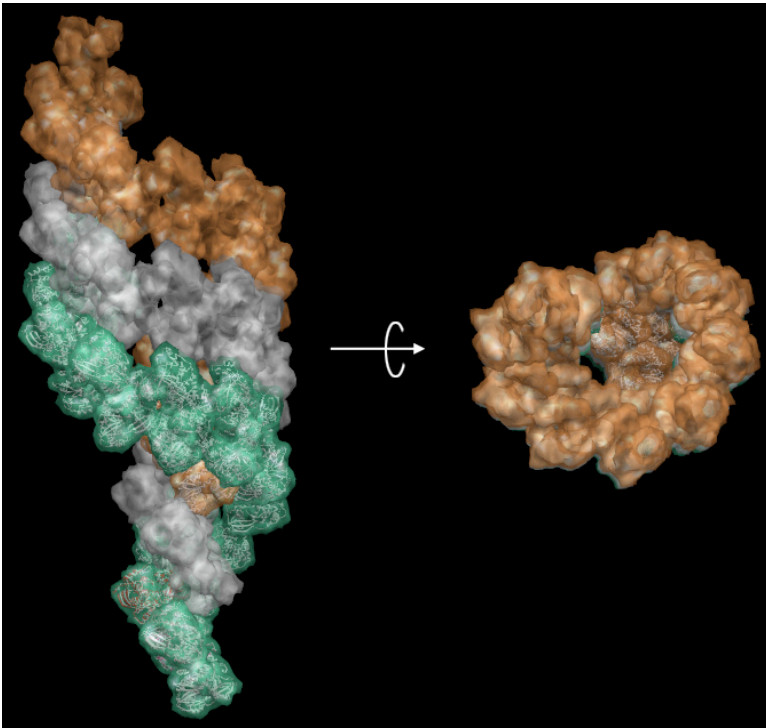
**Supplementary Fig. 1.** *Oligomeric form of purified 3Dpol (Electron micrograph of negatively stained sample). 3Dpol formed short tubes (white arrow) and ribbons (black arrow) after incubation for 5 min at 30 °C. Scale bar 100 nm.*



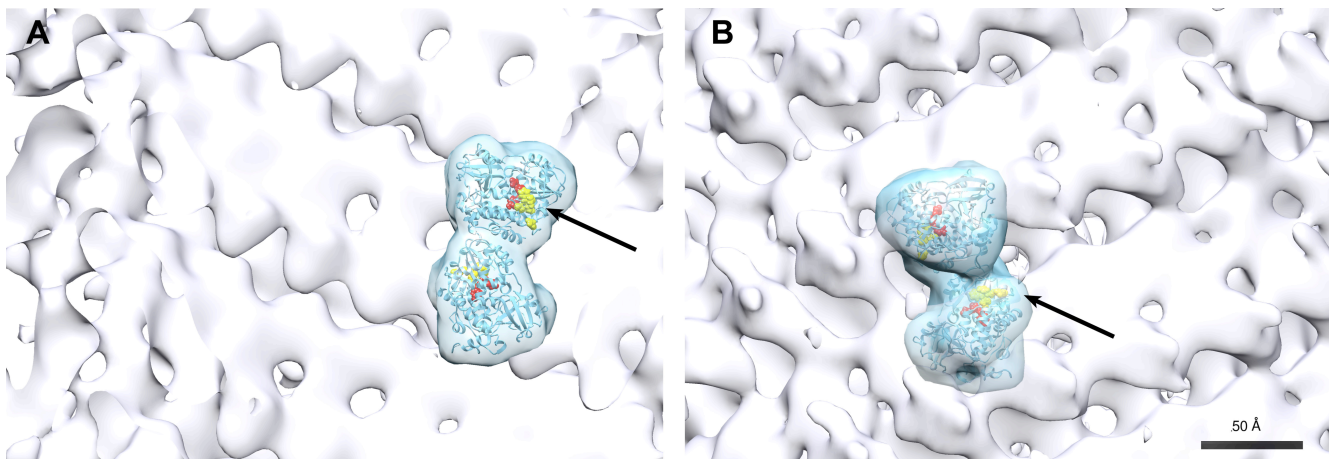
**Supplementary Fig 2.** *Dimensions of unit cells are similar for planar and helical arrays of 3Dpol. (a)* The computed Fourier transform (FT) of a 3Dpol planar array, with unit cell parameters  $a=53 \text{ \AA}$  (blue),  $b=87 \text{ \AA}$  (red),  $\gamma = 89^\circ$ . **(b)** The computed FT of a 3Dpol tube belonging to the  $(-32, 6)$  family, with the length of the unit cell vector  $(0, 1)$  that points to the beating layer line  $90 \text{ \AA}^{-1}$  (red). The resulting unit cell size defined by the  $(0, 1)$  and  $(1, 0)$  vectors (blue dotted line) is different than that of the planar arrays. However, the  $(1, 1)$  vector (blue continuous line) of the helical diffraction pattern is  $47 \text{ \AA}^{-1}$  long. The unit cell size is therefore similar to that of the planar arrays when the unit cell is defined by the  $(0,1)$  and  $(1,1)$  vectors, which includes an interaxial angle  $82^\circ$ .

## Supplementary Materials

Surface for Catalysis by Poliovirus RNA-Dependent RNA Polymerase, by Wang, Lyle, Bullitt



**Supplementary Fig. 3.** *Extendability test of 3Dpol tetramer.* Two parallel interface-I dimers predicted by computational modeling were first extended by superimposition along interface-II producing the green strand. Two more strands (gray and orange) were superimposed along interface-I. The complex spirals up with increasing diameter, resembling a waffle cone. This illustrates visually that strict propagation of parallel interface-I dimers does not form planar arrays. However, our new experimental data strongly support a parallel arrangement of interface-I filaments in planar arrays of 3Dpol through quasi-equivalent interactions between subunits.



**Supplementary Fig. 4.** *Potential binding sites for 3Dpol to membrane via membrane-associated 3AB.* There are accessible binding sites for 3AB on both the inside and outside surfaces of polymerase tubes, as seen when a 3Dpol dimer is fitted into the EM map. Known VPg binding

## Supplementary Materials

### Surface for Catalysis by Poliovirus RNA-Dependent RNA Polymerase, by Wang, Lyle, Bullitt

sites on 3Dpol are shown as yellow spheres, and the active sites are shown in red. Magnification bar 50 Å.

Helical Family	# of Tubes	% of Tubes
(-29, 5)	1	2.9
(-30, 5)	2	5.9
(-31, 5)	2	5.9
(-33, 5)	1	2.9
(-31, 6)	2	5.9
(-32, 6)	9	26.5
(-33, 6)	3	8.8
(-34, 6)	6	17.6
(-36, 6)	1	2.9
(-30, 7)	2	5.9
(-32, 7)	1	2.9
(-35, 7)	1	2.9
(-33, 8)	1	2.9
(-36, 8)	2	5.9

**Supplementary Table.** *Helical families of poliovirus polymerase tubes.* Symmetry was determined for 34 tubes imaged by cryoEM. The majority of tubes were of the (-32,6) or (34,6) family.